SCIENTIFIC REPORTS

SUBJECT AREAS:
COMPUTATIONAL BIOLOGY
BIOLOGICAL MODELS
CELL SIGNALLING
SYSTEMS BIOLOGY

Received
10 April 2012

Accepted
14 August 2012

Published
31 August 2012

Correspondence and requests for materials should be addressed to M.-H.S. (sungm@mail.nih.gov)

Nonlinear Dependencies of Biochemical Reactions for Context-specific Signaling Dynamics

Myong-Hee Sung & Gordon L. Hager

Laboratory of Receptor Biology and Gene Expression, National Cancer Institute, National Institutes of Health, Bethesda, MD 20892, USA.

Mathematical modeling can provide unique insights and predictions about a signaling pathway. Parameter variations allow identification of key reactions that govern signaling features such as the response time that may have a direct impact on the functional outcome. The effect of varying one parameter, however, may depend on values of another. To address the issue, we performed multi-parameter variations of an experimentally validated mathematical model of NF-κB regulatory network, and analyzed the inter-relationships of the parameters in shaping key dynamic features. We find that nonlinear dependencies are ubiquitous among parameters. Such phenomena may underlie the emergence of cell type-specific behaviors from essentially the same molecular network. Our results from a multivariate ensemble of models highlight the hypothesis that cell type specificity in signaling phenotype can arise from quantitatively altered strength of reactions in the pathway, in the absence of tissue-specific factors that re-wire the network for a new topology.

Mathematical modeling of cell signaling pathways is recognized as an important component of molecular systems biology[1–6]. However, it is still a long way before the approach is widely accepted and utilized in mainstream cell biology. This could be attributed to several things. Models are often represented by time-dependent equations that contain kinetic parameters, and most of these rate constants are unknown. One can attempt to estimate some of the constants by in vitro assays, but it is not clear how they approximate the in vivo values. Other rate constants are simply not feasible to measure directly and need to be inferred. Therefore, quite often it is judged that mathematical modeling of a pathway is likely to produce a 'wrong' model, because it is impossible to determine all rate constants accurately.

So how can one avoid using wrong models? A most relevant clue may come from the experimental counterpart: biological results do not come from studying the behavior of one cell. Even in single cell experiments, a finding is confirmed to be definitive if it is reproduced in a large number of cells. Thus, it would be more appropriate to consider an ensemble of models that occupy a 'cloud' of multi-parameter space and correspond to the natural variability of the biological system, rather than looking for 'the correct model' (with a single set of parameter values). Exploration of a range of possible parameter values is necessary not only because of the uncertainty in the model parameter values that were inferred or compiled from diverse sources. But also, individual cells are likely to have slightly variable rate constants for any molecular process in the model[7]. Moreover, studying the parameter space helps understand all the possible behaviors that could be realized under certain pathological or distinct situations.

Here we applied these principles to the widely studied NF-κB pathway and considered an ensemble of models and their signaling characteristics. We present theoretical evidence that context-specific signaling behavior can emerge from parameter dependencies inherent in the nonlinear network of molecular interactions. Our results also imply the existence of situations where reaction kinetics can have discrepant signaling roles in different cell contexts.

Results

NF-κB as a prototypic signaling system within a complex network. NF-κB is an example of latent transcription factors that respond to cell stress and operate in a feedback-controlled network[8–10]. It regulates numerous cell signaling processes and its activity is controlled in part by the level of nuclear translocation. In resting cells, the predominant dimer p65:p50 exists mostly as a cytoplasmic complex bound to its inhibitor IκB proteins.

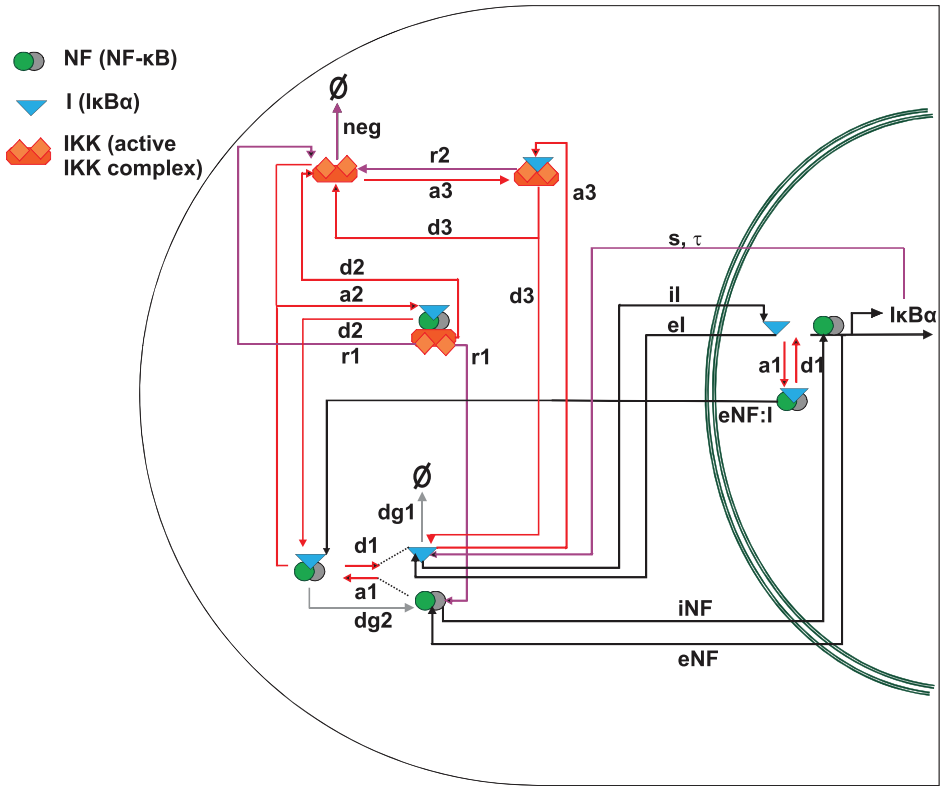

Figure 1 | A mathematical model of the core regulatory network for NF-κB. The process diagram represents the individual reactions included in our model. It includes essential regulatory events such as IKK activation, inducible/constitutive degradation of IκBα, nuclear import/export, inducible synthesis of IκBα, and post-stimulus attenuation of IKK activity. The quantitative model is described in full by the differential equations in Table 1. The arrows are color-coded based on the reaction type (black: transport, red: complex formation, gray: degradation, purple: multiple molecular processes).

Numerous upstream signals induce degradation of the IκB proteins following phosphorylation by the IκB kinase complex (IKK). This release from latency allows NF-κB to translocate into the nucleus and activate expression of target genes, including several feedback genes[8,11].

We used a previously published model of NF-κB that captures experimentally observed behaviors reasonably well[12–14]. The mathematical model includes the core NF-κB regulatory network that operates in virtually all cell types (Fig. 1, Tables 1 and 2). Diverse upstream signals that activate the canonical NF-κB pathway converge at the IKK complex. It consists of catalytic subunits IKKα and IKKβ, and the regulatory subunit NEMO. The 'IKK' in the model corresponds to the active form of IKK, as it has different kinase activities depending on many factors such as its phosphorylation status. The input 'IKK' is introduced as an approximate step function in later simulations. All the processes that negatively regulate IKK activity are combined into a first order term with rate constant neg. The IKK-initiated processes, IκBα phosphorylation at serines by IKK, ubiquitination, and degradation of IκBα by the proteasome is lumped into a single catalytic reaction with constant r_1. r_2 is for a similar but less efficient reaction that targets free IκBα. IκBα binding to NF-κB, and IKK binding to NF-κB-bound or free IκBα, are all reversible reactions with association and dissociation rates that are roughly based on their binding affinities. dg_2 and dg_1 denote parameters for the constitutive degradation of NF-κB bound and free IκBα, respectively. The nuclear import and export of NF-κB, IκBα, and the complex are included as first order terms. Finally, the induction of IκBα gene by NF-κB is represented by a first order process with a rate constant s and a time delay τ. The delay allows one to incorporate multiple processes during the de novo IκBα synthesis (gene transcription, mRNA processing and export, translation, folding, etc.) into a single term, thereby avoiding unnecessary model complexities that would arise from numerous unknown kinetics involving the intermediates.

A multivariate ensemble of mathematical models for NF-κB in the high-dimensional parameter space. We explored our differential equations model with an extensive multi-parameter sampling approach. Instead of varying one parameter at a time while fixing all the others, which results in an extremely limited investigation of the system properties, we employed a large set of random parameter combinations for model simulations. Such a high-dimensional ensemble of parameter states better recapitulate the true variability within a population of single cells, because individual cells are unlikely to have identical values for any rate constant. In fact, typical single cell measurements from flow cytometry or quantitative microscopy result in a distribution, not a single value. Each parameter was allowed to vary by two orders of magnitude, and 1000 random combinations of parameters were generated by Latin Hypercube sampling method for computational efficiency (see Methods for details).

The randomly generated parameter sets were used to solve the delay differential equations where IKK is activated at $t = 0$ and to obtain our multi-parameter variation results. Because of the significant coverage of the high dimensional parameter space, the simulated time course profiles consisted of remarkably diverse response patterns (Fig. 2A), providing numerous signaling dynamics that are possible and may be realized in some cellular and microenvironmental contexts.

Control parameters that influence characteristic features of signaling dynamics. To identify the parameters that influence NF-κB signaling dynamics, we examined the sensitivity of four defining characteristics in a temporal profile of free nuclear NF-κB (see

Table 1 | Differential equations for modeling the core NF-κB network. The 9-variable, 18-parameter delay differential equations model was adapted from[21] with the addition of a term that represents the post-stimulus attenuation of IKK activity ('neg IKK' for the equation for IKK). (Variable definitions: NF = NF-κB, I = IκBα, IKK = the active IKK complex, the colon indicates a bound complex, and the subscript 'n' denotes nuclear species.)

$$\frac{dNF}{dt} = -a_1 NF \cdot I + d_1 NF : I + r_1 NF : I : IKK + dg_2 NF : I - i_{NF} NF + e_{NF} NF_n$$

$$\frac{dI}{dt} = -a_1 NF \cdot I + d_1 NF : I - a_3 I \cdot IKK + d_3 I : IKK + sNF_n(t-\tau) - dg_1 I - i_I I + e_I I_n$$

$$\frac{dNF : I}{dt} = a_1 NF \cdot I - d_1 NF : I - a_2 (NF : I) \cdot IKK + d_2 NF : I : IKK - dg_2 NF : I + e_{NF:I} NF_n : I_n$$

$$\frac{dNF_n}{dt} = -a_1 NF_n \cdot I_n + d_1 NF_n : I_n + i_{NF} NF - e_{NF} NF_n$$

$$\frac{dI_n}{dt} = -a_1 NF_n \cdot I_n + d_1 NF_n : I_n + i_I I - e_I I_n$$

$$\frac{dNF_n : I_n}{dt} = a_1 NF_n \cdot I_n - d_1 NF_n : I_n - e_{NF:I} NF_n : I_n$$

$$\frac{dIKK}{dt} = k(t) - negIKK - a_2 (NF : I) \cdot IKK + (d_2 + r_1) NF : I : IKK - a_3 I \cdot IKK + (d_3 + r_2) I : IKK$$

$$\frac{dI : IKK}{dt} = a_3 I \cdot IKK - (d_3 + r_2) I : IKK$$

$$\frac{dNF : I : IKK}{dt} = a_2 (NF : I) \cdot IKK - (d_2 + r_1) NF : I : IKK$$

Fig. 2B), against variations in parameter values. We will consider F_1, the integrated activity, which is the area under the time course curve divided by the time interval. It is also mathematically equivalent to the time average response. The first response magnitude F_2 is simply the height of the first peak. F_3, the response time, is the time from the onset of stimulation to the first peak. F_4 is the period of oscillation if the temporal profile is periodic. These features capture some essential aspects of a temporal profile.

To assess sensitivity of feature F_k (k = 1, …, 4) against variations in parameter p_i (i = 1, …, 18, as ordered in Table 2), we binned the parameter vectors in the high dimensional parameter space, according to their p_i values (regardless of the other parameter values). Bin-average F_k values were obtained and the standard deviation of these values across the bins was taken to be our sensitivity measure $\Delta_i F_k$. Table S1 shows the parameters sorted by this measure, i.e. how much each parameter influences F_k.

Parameter dependencies are prevalent. Next we addressed our main question by determining whether the influence of a parameter on F_k depends on another parameter. We first illustrate some cases of control parameter pairs with a strong interaction in Fig. 3 (using InterF below; see Methods). Panel A shows how the integrated activity F_1 was influenced by rates of IKK association to NF-κB:IκBα complex (a_2) and IKK-induced phosphorylation/degradation of NF-κB bound IκBα (r_1). Their relationship represented by the best-fit surface indicates that F_1 is a decreasing function of r_1 for low a_2 values, but F_1 is roughly a parabola for high a_2. This can be interpreted in biological terms as follows. First, the integrated activity of NF-κB over time is a most likely determinant of the transcriptional output of direct NF-κB-dependent genes[12]. Then panel A implies that the gene output can be greater for slower signal-dependent degradation of IκBα when IKK binding to substrate is relatively slow. But in a different cellular context where substrate recognition of IKK is faster (due to local tethering, for example),

Table 2 | Description of model parameters and their reference values. The table describes all the molecular processes that are represented in the model and the reference values for the corresponding parameters. All values are from[14] except for the following: τ, neg, and s are parameters for simplifying terms that represent multiple biochemical processes. Therefore, their values were estimated arbitrarily so that the TNF-α response profile from these reference parameter values was qualitatively similar to the experimentally observed time course[12]

Parameter	Reaction type	Biochemical reaction	Reference value	Unit
a_1	complex formation	NF + I −> NF:I	30	μM^{-1} min^{-1}
a_2	complex formation	NF:I + IKK −> NF:I:IKK	11.1	μM^{-1} min^{-1}
a_3	complex formation	I + IKK −> I:IKK	1.38	μM^{-1} min^{-1}
d_1	dissociation	NF + I <− NF:I	0.03	min^{-1}
d_2	dissociation	NF:I + IKK <− NF:I:IKK	0.075	min^{-1}
d_3	dissociation	I + IKK <− I:IKK	0.075	min^{-1}
dg_1	degradation	I −> 0	0.006	min^{-1}
dg_2	degradation	NF:I −> NF	0.0013	min^{-1}
e_{NF}	transport	NF_n −> NF	0.0048	min^{-1}
e_I	transport	I_n −> I	0.025	min^{-1}
$e_{NF:I}$	transport	NF_n:I_n −> NF:I	0.84	min^{-1}
i_{NF}	transport	NF −> NF_n	5.4	min^{-1}
i_I	transport	I −> I_n	0.05	min^{-1}
τ	synthesis	NF_n −> NF_n + I	40	min
neg	inactivation	IKK −> 0	0.002	min^{-1}
r_1	catalyzed degradation	NF:I:IKK −> NF + IKK	11.1	min^{-1}
r_2	catalyzed degradation	I:IKK −> IKK	2.22	min^{-1}
s	synthesis	NF_n −> NF_n + I	0.24	min^{-1}

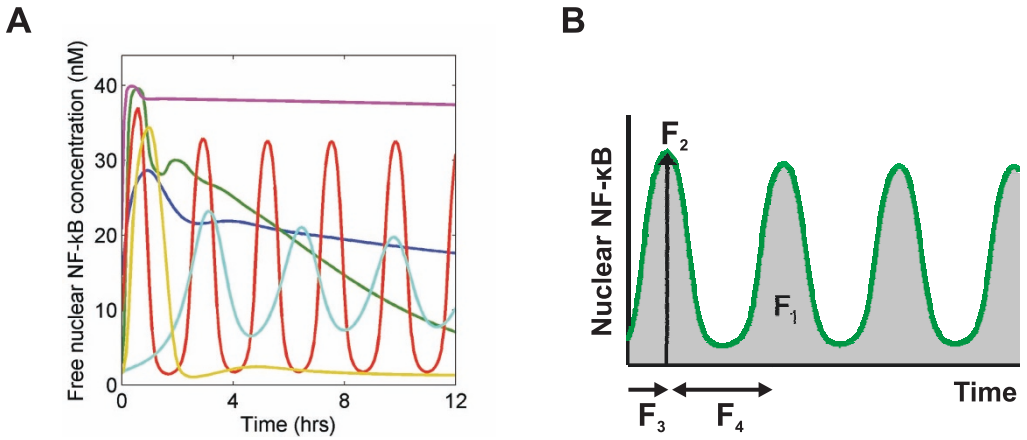

Figure 2 | Multiparameter variation analysis and characteristic measures of signaling dynamics. (A) Six example time course plots from the simulations. The dynamical model was numerically solved for a random sample of 1000 parameter combinations. Each kinetic parameter was varied by two orders of magnitude around the reference value (see Methods). (B) Four defining characteristics of a temporal profile: F_1, F_2, F_3, and F_4 (the period of oscillation if the temporal profile is periodic).

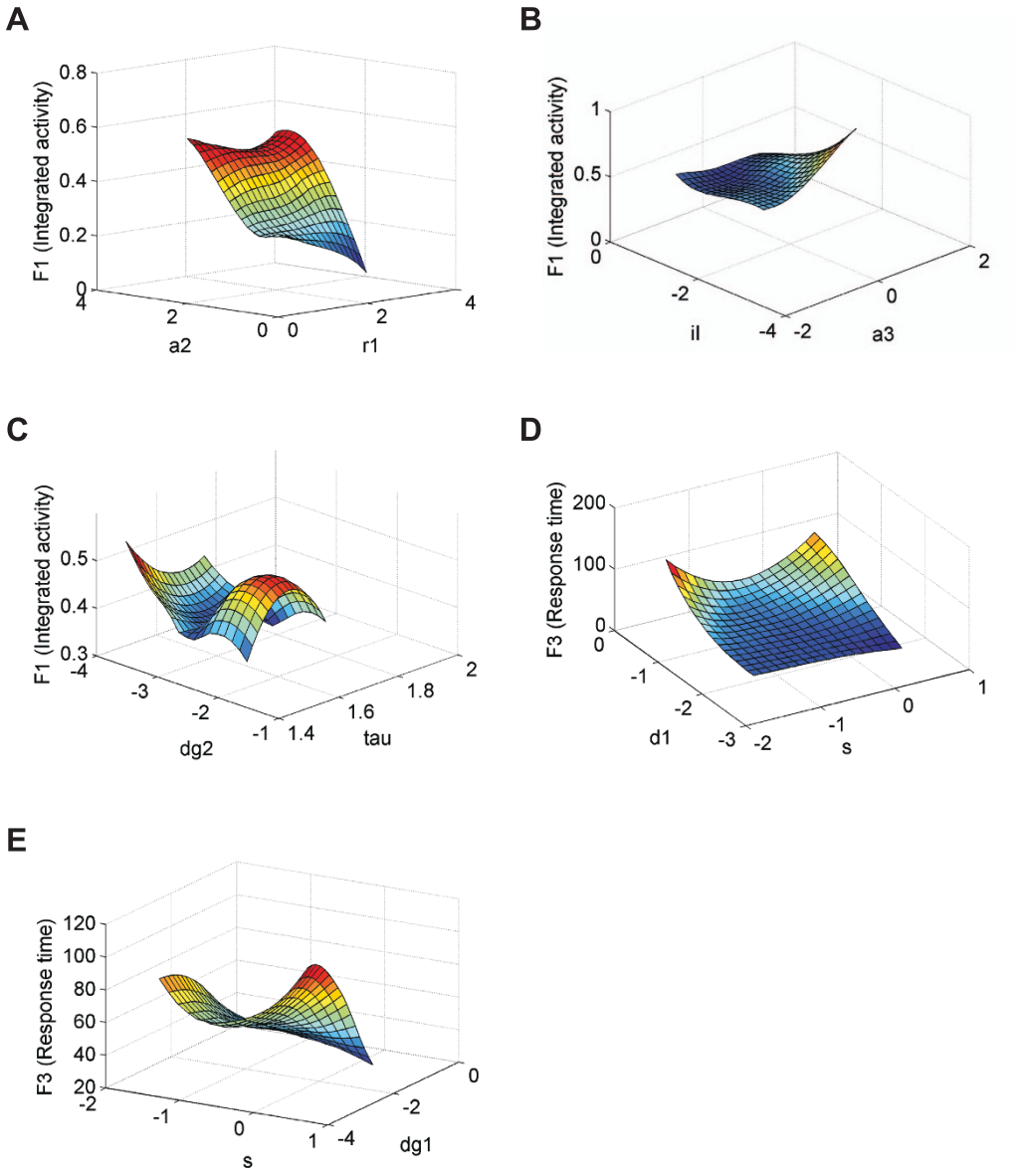

Figure 3 | Nonlinearities in sensitivity of NF-κB signaling characteristics to kinetic parameter values. (A) The surface plot shows the coordinate effect of varying a_2 and r_1 upon F_1. The smooth surface was obtained by locally fitting the individual simulated results (see Methods). The x and y axes are in log10 scale. (B) A similar plot for F_1 against i_1 and a_3. (C) A plot for F_1 against dg_2 and τ. (D) A plot for F_3 against d_1 and s. (E) A plot for F_3 against s and dg_1.

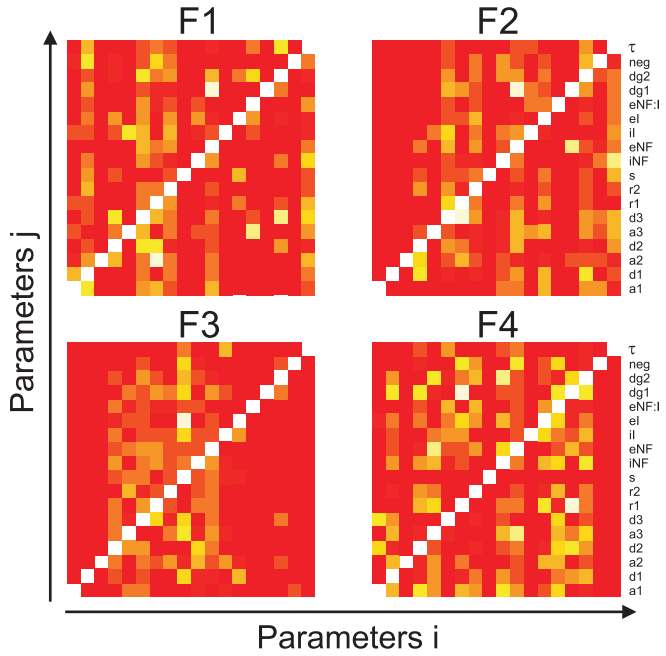

Figure 4 | Parameter dependency map. The color-coded matrix plots display the extent of interaction between all parameter pairs, using the measure InterF (see Methods) for each F_i. The order of model parameters on the axes is the same as in Table 2. The color scale from red to yellow corresponds to low to high interF values.

the transcriptional output may be generally elevated with a slight moderation at a mid-range degradation rate of IκBα.

It is also to be noted that the parameter dependencies are not necessarily symmetric, i.e. the effect of r_1 depended on a_2, but a_2 did not depend on r_1(Fig. 3A). Our simulations also found F_1 to depend on i_I and a_3 in a nonlinear fashion (Fig. 3B). If the import rate i_I was low, F_1 increased with the association rate a_3, but if i_I was high, a_3 had little effect on F_1.

Figure 3C shows another pair of inter-dependent parameters caused by a more complex nonlinearity in their influence on F_1. When the constitutive degradation of NF-κB bound IκBα (dg_2) was minimal, shorter time delays involved in IκBα re-synthesis (τ) resulted in higher integrated NF-κB activity. However, this trend switched to a completely different outcome when the degradation of NF-κB bound IκBα was constitutively higher: There was an optimal time delay that produced maximal transcriptional activity in such a condition. Therefore we conclude that the effect of τ depends on dg_2.

The response time F_3 had differential dependence on d_1 and s in that F_3 was minimized for a distinct value of IκBα synthesis rate s only if d_1, the dissociation rate of NF-κB:IκBα was high (Fig. 3D). Figure 3E indicates that the constitutive degradation of free IκBα (dg_1) affected how the IκBα re-synthesis rate (s) influenced the response time, F_3. If the constitutive degradation was low, the response was fastest at an optimal IκBα induction rate. If, on the other hand, the degradation was constitutively fast, the response was generally fast regardless of the synthesis rate.

Finally, we examined all the inter-dependencies systematically in the following way. For each combination (i, j, k), the coordinate effect of p_i and p_j on F_k was extracted by fitting the data with a smooth surface as shown in Fig. 3. We defined a quantity $InterF_k(i, j)$ to capture the deviation from the independence of p_i effect on F_k from p_j (see Methods). Nonzero $InterF_k(i, j)$ values indicate the presence of an inter-dependency for the two parameters, where the parameter p_i had a different qualitative effect on F_k depending on the value range of p_j. There were numerous such incidences and some pairs (i, j) corresponded to parameters that had weak influences on F_k, where any dependencies would impose an insignificant effect. So, for cases in Fig. 3, we chose those pairs that had significant influence as single control parameters and had high interF values.

We summarize all the results in the 'parameter dependency map' in Fig. 4 (strong to weak interF in yellow to red) which shows the prevalence of inter-dependencies among parameters in shaping the signaling dynamics. Most parameters had differential effects on F_k depending on the values of one or more parameters. On the other extreme, some vertical stretches of red are discernable from the map and correspond to parameters that did not depend on the other parameters. Most of these exert strong control over the relevant F_k. For example, the time delay (τ) and the inactivation rate of IKK (neg) were critical parameters that determine the period F_4 (see Table S1), and their influence on the period were not affected by other parameters.

We explore a possible manifestation of our findings by illustrating a scenario that corresponds to Fig. 3A in more detail (Fig. 5). In mathematical terms, we found that $F_1(r_1)$ is a decreasing function for low a_2 (lower arrow in the surface plot) and is an increasing function for a higher range of a_2 (upper arrow). In biological terms, this implies that the transcriptional consequence of inhibiting signal-induced degradation of IκBα can vary depending on the association rate of IKK to its substrate, NF-κB bound IκBα. This rate, in turn, may well depend on the cell type under study. Cellular features such as the organization and volume of the cytoplasm, or local tethering of kinase scaffolds, are different for distinct cell types. Smaller cytoplasm and local clustering can endow the cells with faster substrate recognition with little need for diffusion-based association. Cell type A represents such a situation. When such cells are treated with an inhibitor that reduces the induced degradation of IκBα, the integrated activity of NF-κB, therefore target gene output, is decreased (indicated by the direction of the upper arrow on the surface plot). However, just the opposite outcome is expected for the same perturbation in another cell type B, where the IKK recognition of its substrate is relatively slow. Other dependencies we found can similarly be elaborated with concrete biological interpretations.

Inter-dependencies of reaction kinetics may well explain, perhaps to a significant extent, the cell type specificity of the signaling roles of numerous factors that seem to have context-dependent actions[15,16]. We note that most signaling pathways possess feedback structures and that the ensuing system nonlinearity is likely to cause inter-dependencies of parameters. To this end, we have looked into another signaling pathway, Wnt/β-catenin, and found a similar extent of parameter dependencies (Myong-Hee Sung, Songjoon Baek, Kwang-Hyun Cho, unpublished data).

Discussion

A significant hindrance in translating the knowledge from a particular quantitative signaling model to a real-world molecular system is the lack of in vivo measurements of the kinetic parameters from the relevant context, such as particular cell lines or primary tissues. We have looked into the effects of varying kinetic parameters upon signaling characteristics and their dependencies on other parameters. For example, suppose that a higher degradation rate of a signaling protein A has the effect of shortening the response time. But this effect may depend on whether the synthesis rate of protein B is within a certain range. The effect of A on response time may even be opposite in other conditions or cellular contexts. By extensive simulations of an NF-κB model, we demonstrate that such a phenomenon can be widespread. This may be a source of apparently discrepant behaviors of the same cellular signaling system in different biological contexts.

The phenomenon seen here may underlie the differential effect of a given molecular process/reaction that is dependent upon distinct levels or efficiencies of another reaction. In general, different cell types are thought to have differences in splice variants[17,18], organiza-

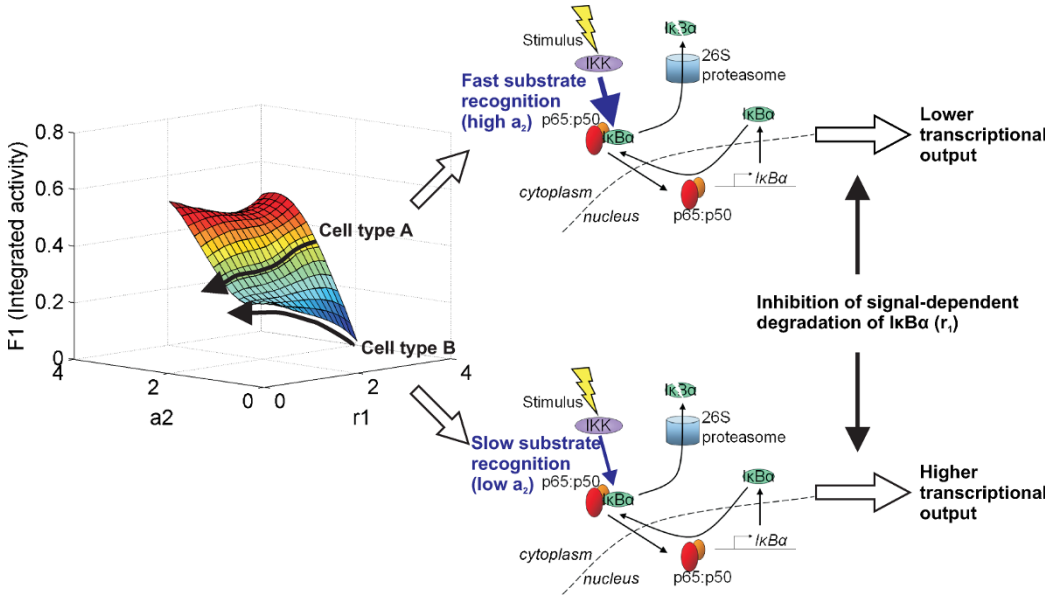

Figure 5 | Biological manifestations: a plausible scenario. Implications from the dependence of r_1, signal-induced degradation of IκBα, on a_2, the association rate of IKK to its substrate, in affecting F_1, the integrated activity of NF-κB. The surface plot is from the result in Fig. 3A. Assuming F_1 is a primary determinant of transcriptional output of NF-κB dependent genes, inhibition of signal-dependent degradation of IκBα (that lowers r_1) has opposite effect on transcriptional output in two cell types A and B, where the IKK substrate recognition is fast and slow (with distinct ranges of parameter a_2), respectively.

tion of the genome into accessible chromatin domains[19], basal turnover of signaling factors, subunit composition of holoenzymes that may affect catalysis rates[20], and more. Here our results explain how quantitative differences in such key molecular systems can lead to qualitatively distinct signaling behaviors.

Methods

A mathematical model of NF-κB signaling network. We used a published mathematical model[12]. Briefly, the delay differential equations (DDE) model described in[21] was modified by including a term (neg in Fig. 1) to represent the inactivation of IKK by various mechanisms including A20, CYLD, and IKK autophosphorylation[11]. These IKK inactivation mechanisms lack single cell data on their kinetic parameters and could not be represented individually. The 9-variable DDE model is shown in Table 1 and the reference parameter values are listed in Table 2.

Multi-parameter variation and model simulations. Each kinetic parameter was varied by 2 orders of magnitude around the reference value (from 0.1- to 10-fold), and was randomly combined with others by the Latin Hypercube sampling method to limit the total number of simulations. The time delay parameter for IκBα synthesis was constrained to vary between 30 and 55 minutes to avoid an unrealistic range. Specifically, parameter combinations were generated by the following procedure. For the j-th parameter, we subdivide the range of the parameter into n (= 5) subintervals of equal size. Then randomly sample n values (p_{ij}, i = 1, …, n), one from each subinterval, for the j-th parameter. The uniform sampling was done on the logscale for all parameters. To combine these values of individual parameters to generate sets of parameter values, we randomly permute the n values for each parameter to get the parameter vectors, i.e. we permute the elements of each column of the matrix p_{ij} separately, and use the rows as the parameter vectors. This sampling method was implemented by the MATLAB function 'lhsdesign' to produce 1000 sets of parameter values. These parameter vectors were used for DDE simulations.

The initial condition for numerical solutions of DDE was provided by specifying a constant history of I = 0.03 μM; NF:I = 0.04 μM; I_n = 0.03 μM; the other variables = 0.

The time delay was given by the parameter τ. All simulations were run by using the MATLAB solver 'dde23' on the time interval [−10 h, 12 h]. IKK activation was introduced at t = 0 by a sharp Gaussian k(t) (standard deviation = 5 min) multiplied by 0.025 μM/min. Evaluation of NF_n from each numerical solution was obtained at the 5 min resolution grid of time points spanning [0 h, 12 h]. The evaluated series $NF_n(t)$ for each simulation was taken as its time course profile for subsequent analyses.

Dynamic measures F_i. For each time course profile, F_i (i = 1, …, 4) values were calculated as follows.

F_1 = ([area under the time course curve]/T)/[total NF],

where T is the time course interval (12 h) and [total NF] is the amount of all NF-containing molecular species (determined by the initial condition and fixed at 0.04 μM). F_2 and F_3 were obtained by finding the first time point t* (> 0) where the time series becomes decreasing, i.e. $NF_n(t^*+dt) - NF_n(t^*) \leq 0$. Then

$F_2 = NF_n(t^*)/[\text{total NF}]$ and
$F_3 = t^*$.

For the period F_4, all time course profiles were analyzed by Fourier analysis to sort for the oscillating profiles. NF_n was considered oscillating if the periodogram from the fast Fourier transform had a detectable peak between 0 h and 5 h either as a global maximum or a local maximum which is at least 0.7 of the global maximum. 345 cases (among 1000) passed the criteria and were used for the analysis of F_4.

Identification of single parameters that control F_i. Given F_i, its sensitivity against varying parameter p_j was measured by $\Delta_j F_i = \sigma(\text{mean}\{F_i(p) \mid p_j \text{ in k-th bin of j-th parameter}\})$ where σ is the standard deviation of bin-averaged F_i values. In particular, p_j was subdivided into 10 bins in log scale, and then all the parameter vectors were binned according to their value range in the j-th dimension. The standard deviation of the bin-average values across the bins was taken as our sensitivity measure $\Delta_j F_i$.

Assessment of pairwise parameter interactions upon F_i. For each F_k - p_i - p_j combination, we extracted the predominant effect of the parameter pairs (p_i, p_j) on F_k by considering a smooth surface fit $z_k(p_i, p_j)$ of the data distribution. This was implemented by Loess fitting F_k against (p_i, p_j) in log scale with a span of 0.5 and by evaluating on a fixed grid of 20 by 20 points over the parameter domain. The p_j-conditional effect of p_i, dF_k, was set to be $(z_k(p_i^{max}, p_j) - z_k(p_i^{min}, p_j))/z_k(p_i^{mid}, p_j)$, where p_i^{max}, p_i^{min}, p_i^{mid} are maximum, minimum, and center grid values of p_i, respectively. The pairwise interaction measure $\text{Inter}F_k(i, j)$ was then defined as

$$\sqrt{-\min\{\max_{p_j}(dF_k)\cdot\min_{p_j}(dF_k),0\}}\ .$$

All Loess-fitting and interaction measures were computed in R (http://www.r-project.org).

1. Suel, G. M., Garcia-Ojalvo, J., Liberman, L. M. & Elowitz, M. B. An excitable gene regulatory circuit induces transient cellular differentiation. *Nature* **440**, 545–550 (2006).
2. Mellman, I. & Misteli, T. Computational cell biology. *J Cell Biol* **161**, 463–464 (2003).
3. Sible, J. C. & Tyson, J. J. Mathematical modeling as a tool for investigating cell cycle control networks. *Methods* **41**, 238–247 (2007).
4. von Dassow, G., Meir, E., Munro, E. M. & Odell, G. M. The segment polarity network is a robust developmental module. *Nature* **406**, 188–192 (2000).
5. Geva-Zatorsky, N. *et al.* Oscillations and variability in the p53 system. *Mol Syst Biol* **2**, 2006 0033 (2006).

6. Longabaugh, W. J., Davidson, E. H. & Bolouri, H. Computational representation of developmental genetic regulatory networks. *Dev Biol* **283**, 1–16 (2005).
7. Voss, T. C. *et al.* Combinatorial probabilistic chromatin interactions produce transcriptional heterogeneity. *J Cell Sci* **122**, 345–356 (2009).
8. O'Dea, E. & Hoffmann, A. The regulatory logic of the NF-kappaB signaling system. *Cold Spring Harb Perspect Biol* **2**, a000216.
9. Escoubet-Lozach, L. *et al.* Mechanisms establishing TLR4-responsive activation states of inflammatory response genes. *PLoS Genet* **7**, e1002401.
10. Siggers, T. *et al.* Principles of dimer-specific gene regulation revealed by a comprehensive characterization of NF-kappaB family DNA binding. *Nat Immunol* **13**, 95–102.
11. Hayden, M. S. & Ghosh, S. Shared principles in NF-kappaB signaling. *Cell* **132**, 344–362 (2008).
12. Sung, M. H. *et al.* Sustained oscillations of NF-kappaB produce distinct genome scanning and gene expression profiles. *PLoS One* **4**, e7163 (2009).
13. Nelson, D. E. *et al.* Oscillations in NF-kappaB signaling control the dynamics of gene expression. *Science* **306**, 704–708 (2004).
14. Hoffmann, A., Levchenko, A., Scott, M. L. & Baltimore, D. The IkappaB-NF-kappaB signaling module: temporal control and selective gene activation. *Science* **298**, 1241–1245 (2002).
15. Chen, F., Beezhold, K. & Castranova, V. Tumor promoting or tumor suppressing of NF-kappa B, a matter of cell context dependency. *Int Rev Immunol* **27**, 183–204 (2008).
16. Dutta, J., Fan, Y., Gupta, N., Fan, G. & Gelinas, C. Current insights into the regulation of programmed cell death by NF-kappaB. *Oncogene* **25**, 6800–6816 (2006).
17. Phair, R. D. *et al.* Global nature of dynamic protein-chromatin interactions in vivo: three-dimensional genome scanning and dynamic interaction networks of chromatin proteins. *Mol Cell Biol* **24**, 6393–6402 (2004).
18. Hoppler, S. & Kavanagh, C. L. Wnt signalling: variety at the core. *J Cell Sci* **120**, 385–393 (2007).
19. John, S. *et al.* Interaction of the glucocorticoid receptor with the chromatin landscape. *Mol Cell* **29**, 611–624 (2008).
20. Burke, P. V. & Poyton, R. O. Structure/function of oxygen-regulated isoforms in cytochrome c oxidase. *J Exp Biol* **201**, 1163–1175 (1998).
21. Sung, M. H. & Simon, R. In silico simulation of inhibitor drug effects on nuclear factor-kappaB pathway dynamics. *Mol Pharmacol* **66**, 70–75 (2004).

Acknowledgements

We thank Alessandra Agresti for helpful discussions. This work was supported in part by the Intramural Research Program of the National Institutes of Health.

Author contributions

M.H.S. designed the study, performed the computation, analyzed results, and wrote the paper. G.L.H. supported the study and commented on the paper.

Additional information

Supplementary information accompanies this paper at http://www.nature.com/scientificreports

Competing financial interests: The authors declare no competing financial interests.

How to cite this article: Sung, M. & Hager, G.L. Nonlinear Dependencies of Biochemical Reactions for Context-specific Signaling Dynamics. *Sci. Rep.* **2**, 616; DOI:10.1038/srep00616 (2012).